A Surface-Driven Polyelectrolyte Reaction Network capable of Molecular Information Processing

A. Hazal Koyuncu,[1,2] Giulia Allegri,[1] Taghi Moazzenzade,[1] Jurriaan Huskens,[1] Saskia Lindhoud[1] & Albert S.Y. Wong*[1,2]

[1] Department of Molecules and Materials & MESA+Institute, University of Twente, Drienerlolaan 5, 7522NB Enschede, The Netherlands

[2] BRAINS (Center for Brain-inspired Nano Systems), University of Twente, Drienerlolaan 5, 7522NB Enschede,The Netherlands

* email: albert.wong@utwente.nl

Abstract

Biochemical communication is ubiquitous in life. Biology use chemical reaction networks to regulate concentrations of myriad signaling molecules. Recent advances in supramolecular and systems chemistry demonstrate that feedback mechanisms of such networks can be rationally designed but strategies to transmit and process information encoded in molecules are still in their infancy. Here, we designed a polyelectrolyte reaction network maintained under out-of-equilibrium conditions using pH gradients in flow. The network, comprises two weak polyelectrolytes (polyallylamine, PAH, and polyacrylic acid, PAA) in solution and one immobilized on the surface (poly-L-lysine, PLL). We chose PAH and PAA as their complexation process is known to be history dependent (i.e., the preceding state of the system can determine the next state). Surprisingly, we found that the hysteresis diminished as the PLL-coated surface supported rather than perturbed the formation of the complex. PLL-coated surfaces are further exploited to established that reversible switching between the assembled and disassembled state of polyelectrolytes can exploited to process signals encoded in the frequency and duration of pH pulses. We envision that the strategy employed to modulate information in this polyelectrolyte reaction network could open novel routes to transmit and process molecular information in biologically relevant processes.

Introduction

Living cells respond to external cues to transmit and process information encoded in small molecules.[1,2] The discovery of recurrent patterns in biology (*i.e.*, network motifs)[3,4] infers that small sets of chemical reaction networks (CRNs) orchestrate spatiotemporal dynamics in and across living cells. Feedback mechanisms in CRNs, essentially, facilitate fast and nonlinear response to stimuli from the environment[5] and systems-level properties such as bistability, oscillations, and homeostasis.[6] Recent advances in out-of-equilibrium networks[7] underline the outstanding successes in systems chemistry in translating the design principles of biological networks into a practical 'chemical programming language'. Strategies to rationally encode, process and integrate chemical signals akin regulatory networks in a living cell, however, remains elusive.[8]

Theory suggests that placing components of CRNs on a surface could create local feedback loops capable of dynamic and spatial aspects of intracellular communication.[9–11] Among other approaches that focus on surface-driven methods to engineer chemical communication,[12] we recently reported a microfluidic strategy that could bestow an acid-base network with the capacity of signal transduction.[13] Briefly, fixating a polyelectrolyte (or more specifically, poly-L-lysine, PLL) on a surface in a microfluidic channel allowed us to work under flow so that the lysine residues can bind and release protons at the liquid-surface interface. The introduction of polyelectrolyte multilayers (PEMs)[14,15] enhanced the rate of

deprotonation of PLL, thereby enabling an output that can be tuned based on the relative timing of input 'spikes' in pH.

Polyelectrolytes (PEs), generally, are well-studied species as they occur wide-spread in living cells to regulate intracellular organization.[16–18] Examples from the past decade[19] and, especially, work from Huck,[20] Spruijt,[21] and Boekhoven[22] highlight how the incorporation of gradients from the environment and dissipation of chemical energy could enable the emergence of systems-level functions (*e.g.*, as self-selection, growth and division, and dynamic phase transitions) from mixtures of polyelectrolytes. Weak PEs are particularly interesting as their tunable charge densities enable reversible switches during a complexation process. How the complexation or assembly of simple poly-acids and bases can be used to transmit information[8] has not been established.

Here, we examine how a polyelectrolyte reaction network is capable of dynamic switching, a feature we consider important for molecular information processing. **Fig. 1** depicts the network motif comprising two weakly charged polyelectrolytes, polyallylamine (PAH) and polyacrylic acid (PAA) and their corresponding polyelectrolyte complex (PAH-PAA). A microfluidic device, with PLL-coated surfaces, was used to perturb this acid-base equilibrium. According to the literature, the complexation of PAH and PAA[23] can display different relaxation times,[24,25] allowing us to investigate how the gradients could influence the history dependency of the polyelectrolyte complex (PEC). We introduced pH gradients to maintain the network under out-of-equilibrium conditions and demonstrated that such gradients allow for finetuning of the assembly and disassembly process during the formation of PECs, impacting how a preceding state of the system can determine the next state. Surprisingly, however, this dependency on the preceding state is lost in the presence of a PLL-coated surface. We demonstrate that the polyelectrolyte reaction network is capable of processing information encoded in the frequency of a temporal signal.

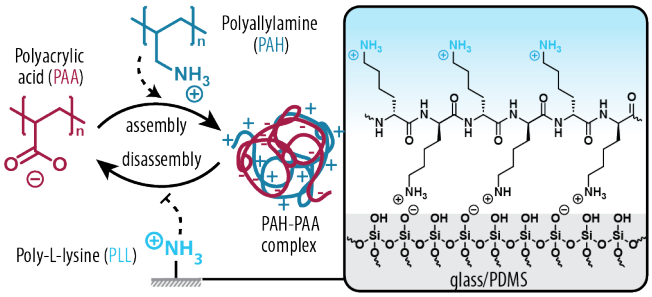

Figure 1. Surface-driven polyelectrolyte reaction network. Network motif with oppositely, and weakly, charged polyelectrolytes that could assemble into a polyelectrolyte complex (PEC). Polyallyl amine (PAH) activates the assembly of PEC (PAH-PAA) by complexing with polyacrylic acid (PAA). The lysine residues (depicted as NH_3^+) are immobilized, prepared by adhering poly-L-lysine (PLL) on the surface inside a microfluidic channel, and inhibit the disassembly of PEC.

Results and Discussion

Polyelectrolyte complexation in flow

We first developed the setup that allowed us to examine PEC formation under flow conditions. Our experimental setup consists of low-pressure pumps that continuously feed a microfluidic channel with PAA and PAH (**Fig. 2a**). The polymers were dissolved in water (with feeding concentrations $[PAA]_{feed}$ and $[PAH]_{feed}$ determined based on their monomer weight, 21 mM) and fed into the microfluidic channel using the syringes mounted on the pumps (see **Methods**). A 1:1 equivalent of PAA and PAH was used to create a charge balance between the polyelectrolytes.[26] Additional syringes with hydrochloric acid ($[HCl]_{feed}$, 10 mM) and potassium hydroxide ($[KOH]_{feed}$, 10 mM) were used to control the pH in the microchannel. The outflow of the channel is connected to an absorbance detector, which we used to measure the transmittance of the solution at 500 nm.[27]

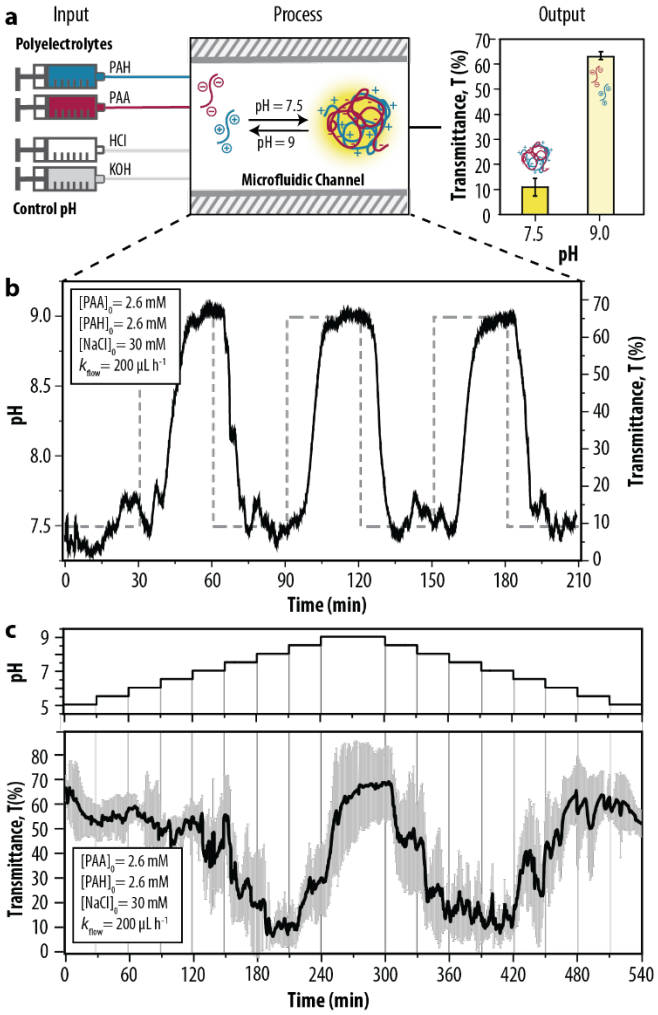

Figure 2. Monitoring PAH-PAA complexation in flow. (a) Schematic representation of the flow setup. Polyelectrolytes and pH are controlled by syringes mounted on low-pressure pumps, and the output is monitored using an absorbance detector (for details, see **Supplementary Information, S4.2**). The low (10%) and high (70%) values at 500 nm indicate the presence and absence of PECs, respectively, with a maximum transmittance (100%) corresponding to water. **(b-c)** Time series showing the trajectory of PEC formation as a function of (b) two pH values (dotted line), and (c) a pH-gradient, established by gradually changing the pH with a step size of 0.5 pH unit per half hour (top graph). The black line depicts the transmittance based on a triplicated experiment (bottom graph). The error bars depict the standard deviation.

Two distinct states were detected: The transmittance is *i)* low when the pH=7.0, and *ii)* high when the pH=9.0 (**Fig. 2a**). A low transmittance (thus, a turbid solution) is indicative of the appearance of PECs, which forms typically at a pH value within the range of an optimal charge density ($6.0 < pH < 8.0$, see SI 3.2). A choice for a pH value outside this range (in the case of pH=9.0) resulted in a high transmittance, indicating that a low amount of the PAH–PAA complex had formed. **Fig. 2b** depicts an experiment wherein we monitored the trajectory of the assembly and disassembly of PECs as a function of the pH. The input pH is kept constant at 7.5 for 30 min to allow the signal to stabilize, after which the pH was changed abruptly to 9.0 and kept, again, constant for 30 min. We repeated these steps three times to determine the steady states at the two pH values, with the average of the observed transmittance depicted in **Fig. 2a**. The screening of other initial conditions (*i.e.*, feeding concentrations of PAA and PAH, salt concentration, and the flow rate) is appended to **Supplementary Information, S4**.

Next, **Fig. 2c** depicts an experiment wherein we gradually changed the pH from 5.0 to 9.0, and *vice versa*. Similar to the previous experiments, we kept each pH value constant for 30 min to ensure that a steady state could be reached before we increased (or decreased) the pH by 0.5 units. Hence, the pH gradient in this experiment is $\Delta pH/\Delta t = 1\ h^{-1}$. **Fig. 2c** shows that the transmittance remained at approximately 70% between 0-120 min (corresponding to a pH change from 5.0 to 7.0) before it decreased

to 5% between 120-210 min. That is, an increase in the pH led to a significant decrease in the transmittance, with the minimum reached at pH 8.0. The high transmittance (~70%) was restored upon a further increase to pH 9.0. The direction of the gradient was changed at t=300 min (returning from pH 9.0 to 5.0), and the same pattern with a minimum in the transmittance around pH=8.0 as well as the recovery of the signal at pH=5.0 was observed. The appearance of both minima in the transmittance confirms that PECs are formed under a pH range wherein both polymers are highly charged. The observation of a robust output demonstrates that the experimental setup can provide a modular approach to examine the formation of PECs in flow.

pH gradients induce the history dependence in polyelectrolyte complexation

Having established the setup, we examined the response of our system to the pH gradient in detail. Notably, the states in **Fig 2** were achieved with a small delay compared to the instance when the pH was changed. That the PEs and PEC require time to be re-dissolved or formed, respectively, provides us with a window wherein we could examine the influence of the gradient on PEC formation. Particularly, the steady states of **Fig. 2c** are visualized by averaging the signal of the last 5 min of each time interval. **Fig. 3a** shows that the local minima, *i.e.*, the point at which the highest concentration of the PAH–PAA complex is formed, are slightly different for the positive ($\Delta pH/\Delta t = +1\ h^{-1}$) and negative gradient ($\Delta pH/\Delta t = -1\ h^{-1}$). Specifically, the PAH–PAA complex was formed at higher pH values for the positive gradient ($7.5 < pH < 8.5$) than for the negative gradient ($6.5 < pH < 8.0$). That the direction of the gradient determined the optimal pH for the PAH-PAA complex suggests that the fate of the complex could depend on a preceding state.

We repeated the experiment but with an increased pH gradient ($\Delta pH/\Delta t = 2\ h^{-1}$, **Fig. 3b** and $4\ h^{-1}$, **Fig. 3c**) to validate this observation, and found three noticeable effects; *i)* the boxes representing the 25-75 percentile of the observed transmittance are narrow (indicating that the final state had stabilized within each step) but broadens when the system is in transition (*i.e.*, the points at which the dashed black line was crossed). *ii)* The difference between the transitions (indicated with closed and open symbols) widens as the gradient increases. *iii)* The local minimum to disappear when we increased the gradient to $4\ h^{-1}$. Hence, not only does the complexation of PAH and PAA and the dissassembly of the complex PAH-PAA occur at different pH values but both processes are highly dependent on the preceding state of the system (*i.e.*, dependent on the direction of the gradient). **Supplementary Information, Fig. S15** validates that this hysteretic behavior can be replicated when the order of the positive and negative gradients is reversed.

A polylysine-coated surface supports rather than perturbs the formation of polyelectrolyte complexes

Next, we examined if the surface-bound poly-L-lysine (PLL) could provide the microfluidic channel with the capacity to further perturb the assembly of PECs. That is, we repeated the experiment with a pH gradient of $4\ h^{-1}$ but using a microfluidic channel with its surface coated with a PLL layer (or, more specifically, a polyelectrolyte multilayer, PEM). We used a three-layered system (PLL-PSS-PLL) as we previously reported that such a polyelectrolyte multilayer (PEM) allows for higher density of PLL on the surface.[13] **Fig. 3d** shows that the transition for the negative gradient did not change and remained at a pH value between 6.0 and 6.5. The transition for the positive gradient (which occurred at a pH value between 6.5 and 7.0), however, was significantly reduced in comparison to the values when the channel was uncoated. Surprisingly, the addition of positively charged polyelectrolytes on the surface did not lead to a perturbed output but instead strengthened the PEC formation and it enabled the PAH–PAA complex to form at a pH closer to the expected optimum.

Intrigued by this phenomenon, we examined the possible deposition of polyelectrolytes from the solution onto the surface using Quartz Crystal Microbalance (QCM, see **Methods**). **Fig. 3e** shows that the frequency continued to decrease when a mixture of PAA and PAH was flown over the PEM-coated surface (solid line). PEM-coated surfaces appeared to enable a continuous build-up of new but surface-bound polyelectrolyte multilayers. This experiment was validated by comparing the obtained results with an uncoated surface (dashed line). In both cases, a Langmuir-shape response did not establish[28], suggesting that a steady state could not be reached within the timescales of our experiments (30 min is the longest time interval used in this study). Instead, a continuous deposition of polyelectrolytes on the surfaces occurred. Thus, both initially uncoated and PEM-coated surfaces can enable a continuous build-up of new surface-bound polyelectrolyte multilayers (or, perhaps, surface-bound polyelectrolyte complexes), with a rate that is higher when the surface was coated with PEMs.[29] The build-up can be prevented using an oligo ethyleneglycol-functionalized PLL[26,28] (PLL-OEG$_{25\%}$, with the 25% indicating the percentage of lysine groups that are functionalized) (dotted line).

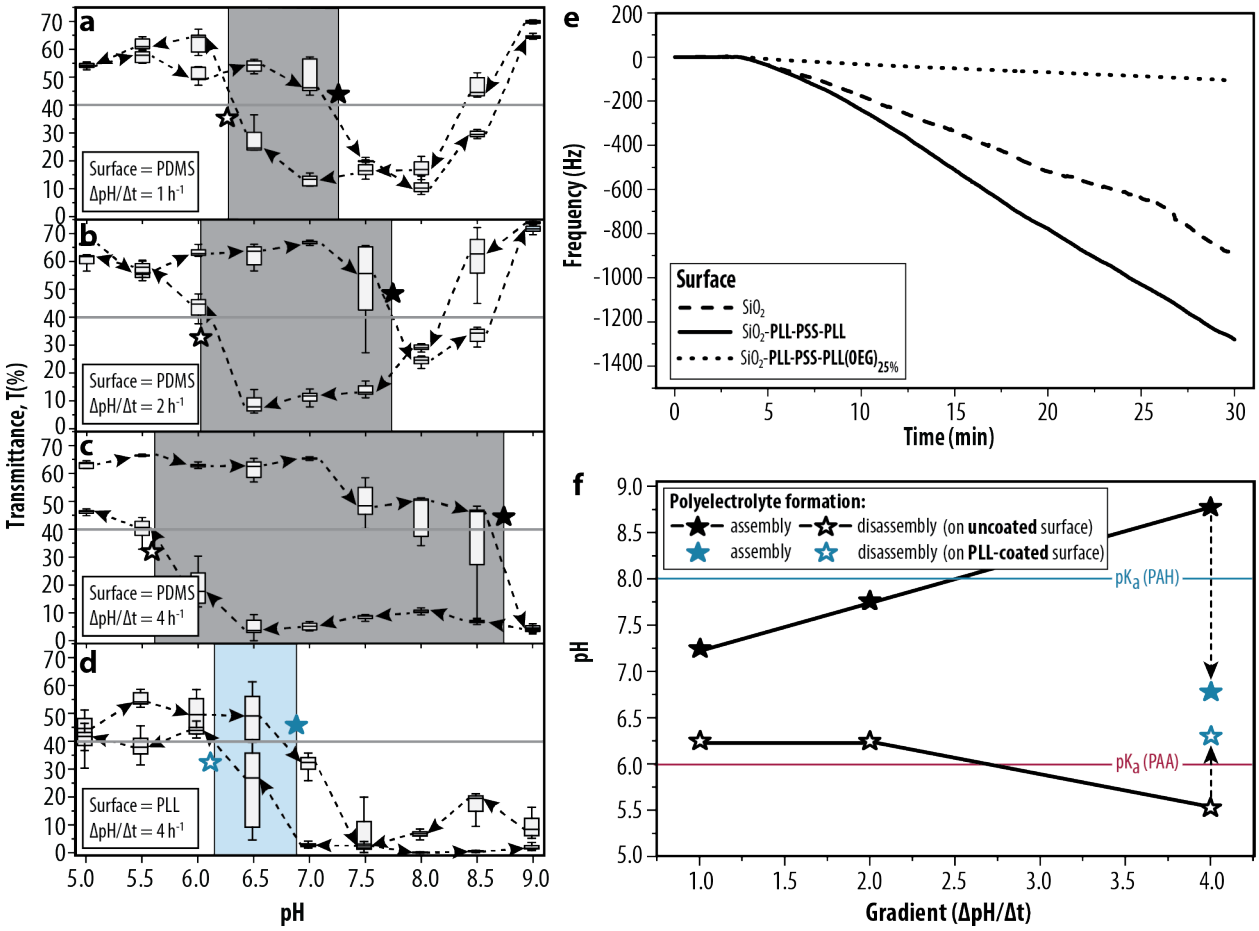

Fig. 3. Examination and validation of gradient- and surface-driven PEC formation. (a-d) Steady-state of the system as a function of the pH gradient (1, 2, and 4 h^{-1}, respectively), examined on uncoated surfaces (a-c) and surfaces coated with PLL (d). The boxplots depict the average of the last 5 minutes of each pH interval. Dash=mean, Box=25-75 percentile, error bars=smallest and largest transmittance of the data set. The grey line at 40% transmittance indicates the transition from a turbid to a transparent solution (**Supplementary Information, Fig. S8**). The time series for **(b-d)** are appended to **Supplementary Information, Fig. S7-S10**. **(e)** The deposition of polyelectrolytes on surfaces was confirmed using quartz crystal microbalance (QCM). The 5th overtone is displayed for change in the frequency, Δf. See **Supplementary Information, Fig. S12** for extended data. Initial conditions: $[PAH]_{feed}$=21 mM, $[PAA]_{feed}$=21 mM, k_{flow}=50 µL min^{-1}. **(f)** Overview of the assembly and disassembly of PEC in the absence and presence of PLL (or, more specifically, PLL-PSS-PLL) at the surface.

Fig. 3f summarizes our findings and shows that the disassembly of PEC occurred under the condition with optimal charge density (pH values between pK_{a1} and pK_{a2}, see **Supplementary Information 3.2**). The assembly of PECs, instead, took place at pH values that increasingly deviated from this region, unless a PLL-coated surface was used. We validated this effect by two additional experiments wherein we changed the third layer of the PEM coating. First, we used a fluorescein 5 isothiocyanate-labeled PLL (PLL-$FITC_{0.3\text{-}1\%}$) as the third layer to examine if PLL could desorb from the surfaces.[30] **Supplementary Information, Fig. S14** shows that the collected output is fluorescently active, confirming that (a trace amount of) PLL-FITC appears to be stripped of the surfaces as charged species, travel through the microfluidic channel. Second, we repeated the experiment with a pH gradient of 4 h^{-1} with PLL-$OEG_{25\%}$ as the third layer to show that the history-dependency in PEC formation can be established on a coated but effectively uncharged surface. **Supplementary Information, Fig. S17** shows that the complexation of PAH and PAA and the disassembly of PAH-PAA occur at different pH values (5.5, and 9.0), and, thus, confirms that history dependency of the functionalized but uncharged surface is similar to the observed behavior for unfunctionalized surfaces. How exactly PEM-coated surfaces could provide a mechanism to temporarily retain polyelectrolyte complexes in the microfluidic channel and thereby support the formation of PECs is beyond the scope of this work. A thorough investigation of the mechanisms underlying our observations would require more details on the types of PECs in the solution[23] and their affinities with the surface-bound PEM. Overall, our observations show that PLL-coated surfaces can allow the polyelectrolytes to adsorb onto, and PLL to desorb from, the surfaces, thereby supporting rather than perturbing the formation of PEC.[31,32]

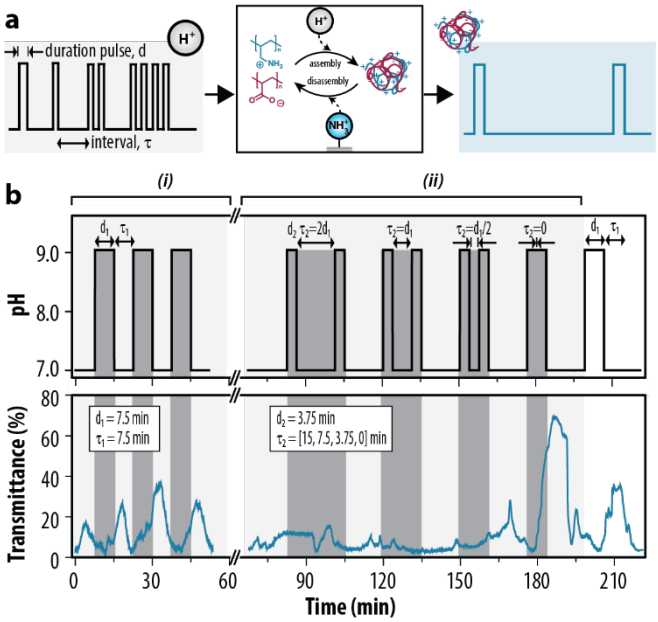

Figure 4. Event-driven signal modulation based on PEC formation. (a) Schematic representation of signal modulation with the polyacid-base network. The spiked input is determined by the duration of, and interval between, pulses in pH. **(b)** Experiment determining temporally sparse activity based on PEC formation. Two pulse conditions were used and indicated using *(i)* and *(ii)*. The pulses are highlighted in grey. Initial conditions: $[PAA, PAH]_0$ = 2.6 mM, flow rate = 200 µL h^{-1}. The surface of fluidic channels is coated with a PEM consisting of PLL-PSS-PLL layers. The transmittance signal at 500 nm (blue line) shows the formation of PEC, with the local maxima indicating the absence thereof.

Signal modulation in a polyelectrolyte reaction network

Finally, we examined if the surface-bound polyelectrolyte can also be exploited for conveying information dependent on pulse arrival time.[8] **Fig. 4a** shows a sequence of hypothetical input pulses with a fixed duration, d, and a decreasing interval between them τ. Inspired by approaches commonly applied in neuromorphic computing,[29,30] we created a temporally sparse input (with the pH based on the results in **Fig. 3d**). **Fig. 4b** shows the input spikes as pulses wherein the pH was changed from 7 to 9, initially

with a duration, d_1, and an interval, τ_1, of 7.5 min (indicated with *i*) and subsequently with a duration that was half of its original value ($d_2=d_1/2$) and a decreasing interval, τ_2, from $2d_1$ to $0d_1$ (indicated with *ii*). We thus examined how the increase of the frequency between the pulses could establish an event-driven output. The output corresponding to the pulse sequence d_1 is fluctuating irregularly, with local maxima between 18-40% transmittance, but nonetheless shows that PECs are formed at an interval similar to τ_1. PECs, however, cannot form if the duration is changed to d_2. No response occurs in the system, unless the duration between pulses was decreased to $\tau_2=d_1/2$. The original signal was restored at $\tau=0d_1$. Hence, PEM-coated channels can be used to examine a complexation process that is defined by the shape of the input curve, opening routes for modulating dynamics—encoded in the frequency and duration, or other features, of a temporal signal—of other biologically relevant processes.

Conclusion

We used weak polyelectrolytes (polyallyl amine, PAH, and polyacrylic acid, PAA) to demonstrate that their complex formation can be controlled under out-of-equilibrium conditions. We hypothesized that a surface-bound polycation, poly-L-lysine (PLL), would increase the history dependence of the PEC as it mainly influences the process that relied on the positively charged polymer. The presence of PLL enhanced the continuous adsorption of either PAA, PAH or the complex PAH-PAA and, instead, supported rather than perturbed the assembly of the PEC. The role of the surface was further exploited for molecular information processing, which we demonstrate by transforming a temporary sparse input pH to a spiked output based on PEC.

The method applied in this work to create surfaces- and gradient- controlled PECs can be logically extended to other compositions of polyelectrolytes.[31] Continuous perturbation of acid-base equilibria based on various PEs, in particular, could reveal how temporal signals of other, more, biologically relevant processes can be modulated using the amplitude, frequency, and duration of an input signal under out-of-equilibrium conditions. We fully expect that the modular means of our setup offers ample opportunities to exploit properties that favors polyelectrolyte-based systems for the design of surface-driven CRNs. Beyond, the simple means by which their complexation can be examined in flow could impact a wide-range of studies from exploring concepts in the origin of life[18] to developing smart materials.[31]

Methods

Chemicals. Chemicals were obtained commercially and used without purification. Potassium hydroxide (KOH, c.a 85%) was purchased from Acros Organics and hydrochloric acid solution (HCl, 32%) was purchased from Merck. Poly(allylamine hydrochloride) (PAH, MW 17.5 kDa) was purchased from Sigma Aldrich. Poly(acrylic acid sodium salt) (PAA, MW 6 kDa) was purchased from Polysciences. Poly-L-lysine hydrobromide (PLL, 15-30 kDa) and poly-L-lysine hydrobromide labeled with fluorescein-5-isothiocyanate (PLL-$FITC_{0.3\text{-}1\%,}$ 15-30 kDa) were purchased from Merck. Poly(sodium 4-styrene sulfonate sodium salt, 1000 kDa) (PSS) was purchased from Sigma Aldrich. VeroClear-RGD 810 polymer material was purchased from Stratasys for 3D printing. SYLGARD™ 184 silicone elastomer kit was purchased from Dow. Water is purified using a Millipore Milli-Q lab water system.

Preparation of polyelectrolyte complexes. Stock solutions of the polyelectrolytes were prepared by dissolving each polyallylamine, PAH, and polyacrylic acid, PAA, in Milli-Q water at a final concentration of 0.2 to 2 g L^{-1}. PAA and PAH (2 g L^{-1}, 21 mM based on Mw of monomer units of both polymers) were dissolved separately in Milli-Q water consisting of 30 mM NaCl. HCl (10 mM) and KOH (10 mM) were prepared in Milli-Q water consisting of 30 mM NaCl and used to adjust pH in flow experiments. Sodium chloride (NaCl, 30 mM) was added to stabilize the complexes without which the output signal became more noisy (Supplementary Information, S4).

Fabrication of microfluidic channels. The upper layer of the microfluidic channels was fabricated using a two-step process. The devices were designed in Solidworks® and printed (Stratasys Objet Pro 30 3D-Printer) to yield a mal. A mixture of curing agent with silicone elastomer base (1:10 m/m, degassed in vacuo) was poured into the mal and was allowed to polymerize in an oven at 75 °C for 30 minutes. PDMS was bonded with a glass slide after activation of the surfaces, for which A ZEPTO plasma oven from Diener Electronic was used. Details on the fabrication process can be found in Supplementary Information, S2.

Coating with PEM. The devices consisting of 3 layers of PEMs (PLL-PSS-PLL, PLL-PSS-PLL-FITC, PAH-PSS-PAH, PLL-PSS-PLL-$OEG_{(25\%)}$) were prepared using layer-by-layer deposition. PLL and PSS solutions were transferred (0.5 g L^{-1} in water) into glass syringes and mounted on low-pressure pumps. CETONI Elements software was used to program low-pressure pumps in the PEM deposition experiments. The first layer was coated by transferring PLL solution onto a freshly oxygen-plasma-activated channel. The device was rinsed using water to remove unreacted species. The second and third layers were deposited using PSS solution without any further activation steps. For details, see Supplementary Information 6.3.

Flow experiments. Flow experiments were performed using a flow setup that consists of low-pressure pumps connected to a microfluidic channel. HCl (10 mM), NaOH (10 mM), PAA (21 mM), and PAH (21 mM) were prepared and transferred into glass syringes and mounted on low-pressure pumps and determine the feeding conditions, $[X]_{feed}$. CETONI Elements software was used to program low-pressure pumps in the flow experiments shown in Fig. 2, 3, and 4 (see Supplementary Information S5 for further information on the sequences used in each experiment). The same software was used to analyze the transmittance data (see Supplementary Information S4 for details of the experimental setup).

QCM measurements. Quartz crystal microbalance (QCM) measurements were performed using silicon dioxide (SiO_2)-coated quartz sensors at 22 °C. The sensors were treated with a UV-ozone cleaner for 45 minutes, followed by immersion in a 2% sodium dodecyl sulfate solution for 45 minutes at 37°C, and then subjected to a 5-minute sonication. They were thoroughly rinsed with water and dried using a gentle flow of nitrogen. Subsequently, the sensors were treated again with UV-ozone cleaner for another 45 minutes. We rinsed the sensor surfaces with Milli-Q water, followed by PLL (0.5 g L^{-1} in water), PSS (0.5 g L^{-1} in water), and PLL. The real-time change in frequency and dissipation response between the 3rd and 9th harmonics were analyzed using Q-Sense. The additional experiments were performed using coated sensors to validate binding events in the presence of polyelectrolytes (PAA and PAH) in flow. See Supplementary Information S6 for further information.

Fluorescence measurements. Aliquote (250 µL) was collected manually from the outflow of the designed experiment in the presence of the PEM-coated surface (PLL-PSS-PLL FITC). Subsequently, a fluorescence experiment was carried out by exciting the fluorescein isothiocyanate labeled PLL (PLL-FITC) at 488 nm and recording the corresponding emission intensity in the range of 500 to 800 nm. The excitation and emission slit widths were set to 5 and 10 nm, respectively. See Supplementary Information S6.3 for further information.

Supporting Information

The authors have cited additional references within the Supporting Information.[13,27,33–37]

Acknowledgements

A.S.Y.W. and J. H. supervised the project. A.S.Y.W. and S.L. conceived the project. A.H.K. performed the experiments in flow and fabricated the microfluidic devices. A.H.K. and G.A. performed the control experiments in batch. A.H.K. and T.M. performed the experiments using QCM. A.S.Y.W. and A.H.K. wrote the manuscript. All authors contributed to revising the manuscript. The project is supported by the Netherlands Organization for Scientific Research (NWO, Veni Grant 202.155 to A.S.Y.W.) and

ChemistryNL (CHEMIE.PGT.2023.006 to A.S.Y.W.). S.L. acknowledges the Sectorplan Bèta en Techniek from the Dutch ministry of Education, Culture and Sciences.

Keywords: Chemical Reaction Network • Molecular information processing • Polyelectrolyte complexes • History dependency • Out-of-equilibrium

References

1. J. Y. Chen, C. Hug, J. Reyes, C. Tian, L. Gerosa, F. Fr ochlich, B. Ponsioen, H. J. G. Snippert, S. L. Spencer, A. Jambhekar, P. K. Sorger, G. Lahav, *Cell Reports.* **2023**, *42*, 112252.
2. A. L. Barabási, Z. N. Oltvai, *Nat. Rev. Genet.* **2004**, *5*, 101–113.
3. J. J. Tyson, K. C. Chen, B. Novak, *Curr. Opin. Cell Biol.* **2003**, *15*, 221–231.
4. R. Milo, S. Shen-Orr, S. Itzkovitz, N. Kashtan, D. Chklovskii, U. Alon, *Science* **2011**, *298*, 217–220.
5. A. Walther, *Adv. Mater.* **2020**, *32*, 1–10.
6. B. A. Grzybowski, W. T. S. Huck, *Nat. Nanotechnol.* **2016**, *11,* 585-592.
7. N. Giuseppone, A. Walther, Vol.1 (Eds. N. Giuseppone, A. Walther) *Out-of-Equilibrium (Supra)molecular Systems and Materials*, **2021**, pp. 1–19.
8. J. E. Purvis, G. Lahav, *Cell* **2013**, *152*, 945–956.
9. B. N. Kholodenko, *Nat. Rev. Mol. Cell Biol*. **2006**, *7*, 165–176.
10. G. Menon, J. Krishnan, *Nat. Commun.* **2021**, *12,* 1-21.
11. S. Clamons, L. Qian, E. Winfree, *J. R. Soc. Interface* **2020**, 17, 20190790.
12. J. Ventura, A. Llopis-Lorente, L. K. E. A. Abdelmohsen, J. C. M. van Hest, R. Martínez-Máñez, *Acc. Chem. Res.* **2024**, *57,* 6, 815–830.
13. A. H. Koyuncu, J. Movilli, S. Sahin, D. V. Kriukov, J. Huskens, A. S. Y. Wong, *ChemSystemsChem* **2024**, *6*, e202300030.
14. M. Schönhoff, *J. Phys. Condens. Matter* **2003***,15,* 1781-1808.
15. Ph. Lavalle, C. Gergely, F. J. G. Cuisinier, G. Decher, P. Schaaf, J. C. Voegel, C. Picart, *Macromolecules* **2022***, 35*, 4458–4465.
16. A. S. Lyon, W. B. Peeples, M. K. Rosen, *Nat. Rev. Mol. Cell Biol.* **2021**, *22*, 215–235.
17. S. F. Banani, H. O. Lee, A. A. Hyman, M. K. Rosen, *Nat. Rev. Mol. Cell Biol.* **2017,** *18*, 285–298.
18. E. Spruijt, *Commun. Chem*. **2023**, *6*, 1–5.
19. A. B. Cook, S. Novosedlik, J. C. M. van Hest, *Acc. Mater. Res*. **2023**, *4*, 287–298.
20. E. te Brinke, J. Groen, A. Herrmann, H. A. Heus, G. Rivas, E.Spruijt, W. T. S. Huck, *Nat. Nanotechnol.* **2018**, *13*, 849–855.
21. K. K., Nakashima, M. H. I. van Haren, A. A. M. André, I. Robu, E. Spruijt, *Nat. Commun.* **2021**, *12,* 1-11.
22. N. A. Yewdall, A. A. M. André, T. Lu, E. Spruijt, *Curr. Opin. Colloid Interface Sci.* **2021**, *52*, 101416.
23. Y. Zhang, F. Li, L. D. Valenzuela, M. Sammalkorpi, J. L. Lutkenhaus, *Macromolecules* **2016**, *49*, 7563–7570.
24. S. M. Lalwani, P. Batys, M. Sammalkorpi, J. L. Lutkenhaus, *Macromolecules* **2021**,*54*, 7765–7776.
25. S. Lindhoud, S., W. Norde, M. A. C. Stuart, *J. Phys. Chem. B* **2009**,*113,* 5431–5439.
26. C. R. Kinnane, K. Wark, G. K. Such, A. P. R. Johnston, F. Caruso, *Small* **2009***, 5*, 444–448.
27. J. Movilli, S. S. Choudhury, M. Schönhoff, J. Huskens, *Chem. Mater.* **2020,** *32*, 9155–9166.
28. V. Sze, Y. H. Chen, T. J. Yang, J. S. Emer, *Proc. IEEE* **2017***, 105*, 2295–2329.
29. C. D. Schuman, S. R. Kulkarni, M. Parsa, J. P. Mitchell, P. Date, B. Kay, *Nat. Comput. Sci.* **2022,** *2*, 10–19.
30. V. S. Meka, M. K.G. Sing, M. R. Pichika, S. R. Nali, V. R.M. Kolapalli, P. Kesharwani, *Drug Discov. Today* **2017,** *22*, 1697–1706.

31. J. J. Richardson, J. Cui, M. Björnmalm, J.A. Braunger, H. Ejima, F. Caruso, *Chem. Rev.* **2016***, 116,* 14828−14867.
32. D. V. Kriukov, A. H. Koyuncu, A. S. Y. Wong, *Small* **2022***, 18,* 2107523.
33. P. Li, J. Cogswell, M. Faghri, Sens. Actuator B-Chem. **2012**, *174*, 126–132.
34. M. Lemmers, E. Spruijt, L. Beun, R. Fokkink, F. Leermakers, G. Portale, M. A. Cohen Stuart, J. van der Gucht, *Soft Matter* **2012***, 8,* 104–117.
35. R. Chollakup, W. Smitthipong, C. D. Eisenbach, M. Tirrell, *Macromolecules* **2010**, *43*, 2518–2528.
36. H. N. Po, N. M. Senozan, *J. Chem. Educ.* **2001**, *78*, 1499–1503.
37. R. Chollakup, J. B., Beck, K. Dirnberger, M. Tirrell, C. D. Eisenbach, *Macromolecules* **2013**, *46*, 2376–2390.